

## STUDY OF THE INFLUENCE OF Na/Li ON THE MICROSTRUCTURE OF AN ALUMINOSILICATE NUCLEAR GLASS

DALILA MOUDIR<sup>1\*</sup>, NOUR EL HAYET KAMEL<sup>1</sup>, ABD EL BAKI BENMOUNAH<sup>2</sup>, SOUMIA IKHADDALENE<sup>3</sup>,  
YASMINA MOUHEB<sup>1</sup>, FAIROUZ AOUCHICHE<sup>1</sup>

<sup>1</sup>Nuclear Research Center of Algiers, Nuclear Technology Division, 2. Bd Frantz Fanon, BP 399, RP-Algiers, Algiers, Algeria

<sup>2</sup>Unit, Process Materials and Environment, University M' Hamed Bouguara, Boumerdes, 35000, Algeria

<sup>3</sup>Faculty of Science, Department of Chemistry, Railway Station Road - 35000 Boumerdes, Algeria

*An aluminosilicate nuclear glass storage was synthesized by a double melting method and characterized using both X-ray diffraction and scanning electron microscopy (SEM) techniques. Physical parameters like density and molar volume were measured. Fourier Transform Infrared Spectroscopy (FTIR) confirms the glass chemical composition. Differential thermal analysis (DTA) was used to determine the glass-transition temperature (T<sub>g</sub>). Samples microstructure was also characterized by Vickers microhardness, young's modulus and electrical resistivity.*

**Keywords:** nuclear glass, storage, SEM, DTA, FTIR

### 1. Introduction

Glass matrices are presently used as non-specific nuclear waste confinement matrix, due to their properties, such as a good structural flexibility to incorporate large amounts of the most hazardous radionuclides in high level waste (HLW) and fission products solutions, simplicity in processing technique, high corrosion resistance, good thermal and radiation stability, and inexpensive raw materials [1].

Aluminosilicate glasses have the capability to retain radioactivity for long duration times. Their compositions vary with the composition of the various wastes, which in turn depends on the reactor type, the cooling of spent fuel, etc. [2]. Although, the glass basic network is composed of Si and Al oxides. Various alkaline or alkaline-earth elements are used as modifiers, and are known to decrease significantly the glasses melting temperatures. Several radioactive elements, with given concentrations, coming from the radioactive waste can be incorporated in the glass, as lanthanides and fission products (or radioactive transition metals: Mo, Mn, Cd, Gd, La, Ni, Zn, Y, Nd, etc.) [1 - 4].

Such confinement glassy matrix is called: a nuclear glass.

Many physical properties associated with the alkali ion movement and structure of the alkali oxide containing glasses show a non-linear behavior

exhibiting a minimum or maximum, as a function of alkali content, if one alkali ion is gradually replaced by another alkali ion, keeping the total alkali content constant. This behavior is called the "mixed alkali effect" (MAE) [5, 6].

The most evident manifestation of this effect has been observed in DC electrical conductivity and in the activation energy exhibiting a deep minima and maximum as a function of composition in the intermediate ratio of alkali ions [7].

In this study, we investigate the influence of the mixed alkali effect on the structural, physico-chemical, thermal, mechanical and electrical properties of an aluminosilicate glass based on the system SiO<sub>2</sub>-Al<sub>2</sub>O<sub>3</sub>-Fe<sub>2</sub>O<sub>3</sub>-MgO-Li<sub>2</sub>O-Na<sub>2</sub>O-K<sub>2</sub>O-Y<sub>2</sub>O<sub>3</sub>-ZrO<sub>2</sub>-La<sub>2</sub>O<sub>3</sub>-MoO<sub>3</sub>. Lanthanum (La) and yttrium (Y) were employed as lanthanide/actinide surrogates. [Na<sub>2</sub>O]/([Na<sub>2</sub>O] + [Li<sub>2</sub>O]) alkali-ratio is ranging between 0.057 and 0.278.

The samples are characterized by their physical, microstructural, mechanical, thermal and electrical properties. The glasses' densities and molar volumes are calculated. The amorphous structure was confirmed by X-ray diffraction (XRD) and scanning electron microscopy (SEM). The chemical composition was confirmed by FTIR analysis, and DTA was used to assess the glass allotropic transformation. The glass structure was also characterized by Vickers microhardness, Young's modulus and electrical resistivity.

\* Autor corespondent/Corresponding author,  
E-mail: dalilamoudir@yahoo.fr

**2. Experimental part**

The glasses were prepared using N. Ollier and al. [8] method, which consists in two melting/casting steps. The following commercial reagents were employed: SiO<sub>2</sub> (PROLABO, Purity ≥ 100%), Al<sub>2</sub>O<sub>3</sub> (FLUKA, Purity ≥ 100%), Fe<sub>2</sub>O<sub>3</sub> (MERCK, Purity ≥ 99%), Na<sub>2</sub>O (MERCK, Purity ≥ 99.5%), K<sub>2</sub>O (MERCK, Purity ≥ 99%), Li<sub>2</sub>O (MERCK, Purity ≥ 99%), MgO (FLUKA, Purity ≥ 97%), MoO<sub>3</sub> (MERCK, Purity ≥ 99.5%), ZrO<sub>2</sub> (ALDRICH, Purity ≥ 99%), La(NO<sub>3</sub>)<sub>3</sub> (FLUKA, Purity 99, 99%), and Y<sub>2</sub>O<sub>3</sub> (MERCK, Purity ≥99%).

Rare earth elements (REE) oxides are dried over night at 1,000 °C, and the other oxides at 400 °C. La<sub>2</sub>O<sub>3</sub> is prepared by calcination at 450 °C of La(NO<sub>3</sub>)<sub>3</sub>. Four powder mixtures were prepared with different [Na<sub>2</sub>O]/([Na<sub>2</sub>O]+[Li<sub>2</sub>O]) molar ratios (Table 1) ranging from 0.057 to 0.278. A batch of 25 g is prepared for each glass. The mixtures are homogenized in an Automatic Sieve Shaker D403 during 7 h to achieve good particles dispersion. The powders mixtures are melted at 1450 °C in air for 1h 30min, in Pt crucibles, in a BLF 1800 Carbolite furnace. The heating step was of 5°C/min. The melted glasses are casted in steel cylindrical molds.

**Table 1**  
Chemical composition of the studied glasses.

[Na <sub>2</sub> O]/([Na <sub>2</sub> O]+[Li <sub>2</sub> O])	0.057	0.121	0.194	0.278
ZrO <sub>2</sub>	4.5	4.5	4.5	4.5
Al <sub>2</sub> O <sub>3</sub>	15.0	15.0	15.0	15.0
MgO	5.0	5.0	5.0	5.0
Na <sub>2</sub> O	2.0	4.0	6.0	8.0
Fe <sub>2</sub> O <sub>3</sub>	2.0	2.0	2.0	2.0
K <sub>2</sub> O	4.0	2.9	0.5	1.0
Li <sub>2</sub> O	16.0	14.0	12.0	10.0
La <sub>2</sub> O <sub>3</sub>	0.5	0.5	0.5	0.5
Y <sub>2</sub> O <sub>3</sub>	0.5	0.5	0.5	0.5
MoO <sub>3</sub>	3.0	3.0	3.0	3.0
SiO <sub>2</sub>	47.5	48.6	51.0	50.5
Total	100.0	100.0	100.0	100.0

**3. Results and Discussion**

**3.1. Physical Characterization**

*Density and molar volume Measurements*

The glasses density was measured by Archimedes method (d), with a hydrostatic balance using distilled water as immersion liquid. The molar volume was calculated using the mathematical formula (1):

$$V_m = \frac{\sum_i X_i M_i}{100 d} \tag{1}$$

With:

M<sub>i</sub>: is the i element molar mass (g/mol), x<sub>i</sub>: the weight fraction of the i oxide (%), and d: the Archimedes density (g/cm<sup>3</sup>).

One can note that the glasses' Archimedes density vary non-linearly with [Na<sub>2</sub>O]/([Na<sub>2</sub>O]+[Li<sub>2</sub>O]) molar ratio. It is maximum for [Na<sub>2</sub>O]/([Na<sub>2</sub>O]+[Li<sub>2</sub>O])= 0.194. Our results are closer to those found in literature.

A. Edukondalu and al. [9] found density values of 2.724 and 2.805 g/cm<sup>3</sup> for a glass in the system xLi<sub>2</sub>O-(30-x) Na<sub>2</sub>O-10WO<sub>3</sub>-60B<sub>2</sub>O<sub>3</sub>.

G. Padmaja and al. [10] reported densities between 2.40 and 2.61 g/cm<sup>3</sup> for an alkali borate glass in the system Li<sub>2</sub>O-K<sub>2</sub>O-ZnO-B<sub>2</sub>O<sub>3</sub>-Fe<sub>2</sub>O<sub>3</sub>.

The glasses molar volumes increase nonlinearly according to the molar ratio. The maximum value (23.43 cm<sup>3</sup>/mol) is found for [Na<sub>2</sub>O]/([Na<sub>2</sub>O]+[Li<sub>2</sub>O])= 0.278.

R. Laopaiboon and C. Bootjomcha[11] found molar volumes of 23.731cm<sup>3</sup>/mol and 23.812 cm<sup>3</sup>/mol for series of glasses in the system xCeO<sub>2</sub>-20Na<sub>2</sub>O-Al<sub>2</sub>O<sub>3</sub>-13B<sub>2</sub>O<sub>3</sub>-6.5CaO-1.5PbO-(58-x)SiO<sub>2</sub> prepared by melting at 1250 °C. Fig. 1 represents the variations of both molar volume and density according to [Na<sub>2</sub>O]/([Na<sub>2</sub>O]+[Li<sub>2</sub>O]) ratio. According to this ratio, the variation of both the molar volume and density is non-linear. The most dense glass is for the ratio [Na<sub>2</sub>O]/([Na<sub>2</sub>O]+[Li<sub>2</sub>O])=0.194. This non-linear behavior is due to changes in [Na<sub>2</sub>O]/([Na<sub>2</sub>O]+[Li<sub>2</sub>O]) ratios. This phenomenon is referred to the mixed alkali effect (MAE). R.L. Myuller [12] reports that the more is the difference between the alkali ions size, the more is MAE effect.

The MAE has been thoroughly studied by N. Ollier and al. [8]. These authors found that the structure depolymerization is a coupling phenomenon between depolymerization and swelling in the glass.

The addition of modifying cations into a silica glass breaks Si-O-Si bonds and creates NBO oxygen, at the rate of one O per M<sup>+</sup> alkaline ion, and two O per M<sup>2+</sup> alkaline earth ion [13].

The modifying ions therefore have the effect of depolymerizing the silicate network, and thus create discontinuities within it, by introducing ionic bonds (M<sup>+</sup> --- NBO or M<sup>2+</sup> --- NBO).

In alkali silicates glasses (Na<sub>2</sub>O, Li<sub>2</sub>O, CsO or K<sub>2</sub>O), one can found NBO oxygen in the neighborhood of alkaline ions. These oxygens cause discontinuities of the silica network. The bond between alkaline and oxygen NBO is essentially ionic, and therefore much weaker than the covalent siloxane bond.

Na chains reduce polymerization between silica tetrahedra, and are preferred sites for fracture and dissolution [14].

The size and nature of the alkaline element are important parameters. I. Yasui et al. [15] demonstrate that sodium had an "ideal" size, close to that of the vacant space between the silicon chains. By this way, sodium can bind both to 3 or 4 oxygen atoms of the Si chain, and to 1 or 2 NBO oxygen atoms. Alkalis smaller than sodium (as Li)

bind with oxygen atoms coming from several different chains. If the alkaline atom size is greater than the optimal size, usually that of K, the silicate polyhedral chains deform to integrate these alkalis in the vacant sites[15]. Therefore, the presence of K in the studied glass system will influence its properties. As a consequence, when K<sub>2</sub>O content decreases ([Na<sub>2</sub>O]/([Na<sub>2</sub>O]+[Li<sub>2</sub>O])=0.194), V<sub>m</sub> increases suddenly, due to the lack in this big ion (K<sup>+</sup> ionic radius=133-140 pm, compared to Na<sup>+</sup> and Li<sup>+</sup> ionic radii which are 95 and 60 pm, respectively). This produces an extent of the glass units.

The alkaline ion sites average potential variation in the mixed glasses is a consequence of a different interaction between the NBO oxygen atoms and the different alkaline ions, which have various ionic radii. The nonlinear variation of the alkali potential sites, in mixed glasses, when one alkaline is replaced by another, would provide a basis for the structural explanation of the MAE effect.

Many authors use the molar volume in oxygen V<sup>o</sup><sub>m</sub>, instead of the molar volume V<sub>m</sub>. V<sup>o</sup><sub>m</sub> expresses the volume occupied by one mole of oxygen atoms [16].

$$V^o_m = \frac{\sum_i X_i M_i}{d \sum_i n_i X_i} \quad (2)$$

With n<sub>i</sub> is the number of oxygen atoms in the base unit of the i oxide.

As an example, the addition of small amounts of Na<sub>2</sub>O to pure silica results in a very small increase of V<sup>o</sup><sub>m</sub>, which means that the Na<sup>+</sup> ions can be inserted into the vacant spaces of the glass network. At a high Na<sub>2</sub>O content, one can note a marked increase in V<sup>o</sup><sub>m</sub> [16].

The incorporation of K element leads to a greater expansion of the glass network, due to the larger ionic radius of this ion. On the other hand, Li curve shows that Li<sup>+</sup> ions insert in the network empty spaces, and provoke network shrinkage [16]. This explains the sharp drop in V<sub>m</sub> when [Na<sub>2</sub>O]/([Na<sub>2</sub>O]+[Li<sub>2</sub>O]) alkali molar ratio is greater than 0.2.

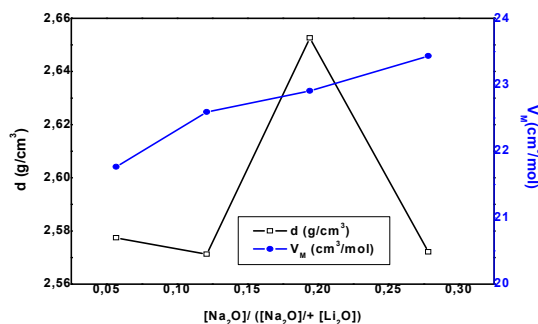


Fig. 1 –Evolution of the glass Archimedes density and molar volume as a function of [Na<sub>2</sub>O]/([Na<sub>2</sub>O]+[Li<sub>2</sub>O]) molar ratio.

### 3.2. Microstructural Characterization X-Ray Diffraction

XRD analysis was performed by means of Philips X'Pert PRO equipment. The result confirms the glasses amorphous structure whatever [Na<sub>2</sub>O]/([Na<sub>2</sub>O]+[Li<sub>2</sub>O]) molar ratio.

A typical diffractogram of the studied glasses is shown in Fig.2.

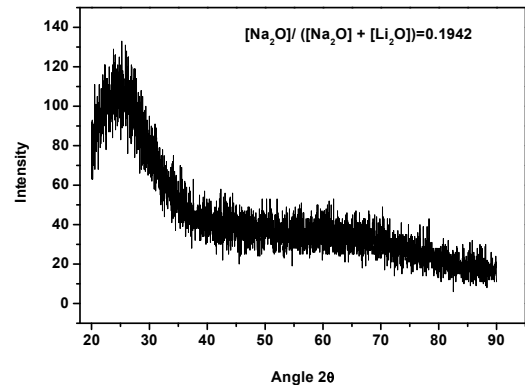


Fig. 2–A typical diffractogram of the synthesized glasses.

### Scanning Electron Microscopy (SEM) Analysis

The glasses microstructure was revealed by both the bulk and surface SEM observations. SEM analysis was performed on a Philips XL30 microscope. A typical micrograph of the studied glasses is shown on Fig. 3. The micrograph confirms the glasses homogeneity for the different [Na<sub>2</sub>O]/([Na<sub>2</sub>O]+[Li<sub>2</sub>O]) molar ratios.

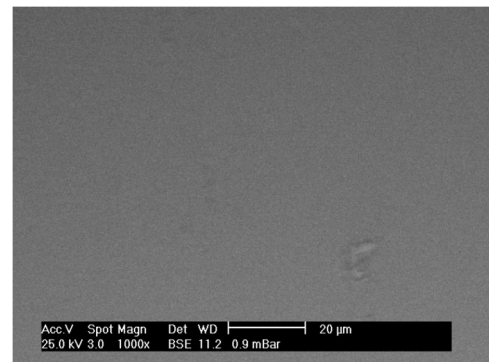


Fig. 3– SEM micrograph of the glass with [Na<sub>2</sub>O]/([Na<sub>2</sub>O]+[Li<sub>2</sub>O])=0.278.

### Fourier Transform Infrared Spectroscopy analysis

FTIR analysis is recorded using a NICOLET 380 spectrometer, in 400-4000 cm<sup>-1</sup> range, at room temperature. FTIR spectra are gathered in Fig. 4. The experimental FTIR data are shown in Table 2.

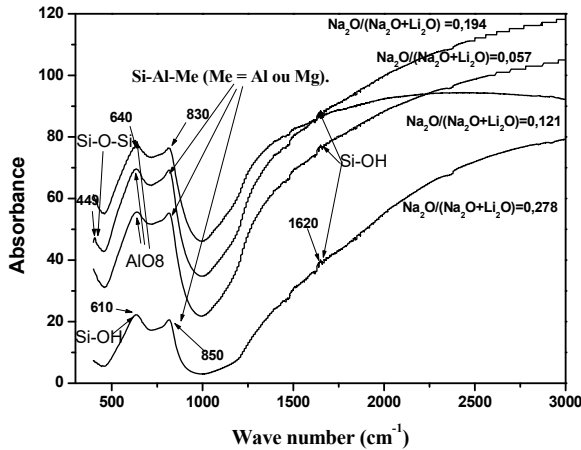


Fig. 4- Glasses FTIR spectra for different  $[Na_2O]/([Na_2O] + [Li_2O])$  ratios.

Table 2

Glasses FTIR main vibration bands.

Vibration Band	Wave number (cm <sup>-1</sup> )	References
Si-O-Si	467- 473	[17]
Si-O	1070	[18]
Na-O, Li-O, K-O	444	[21]
Al-O, Mg-O, Si-O-Me.	700	[25]
Al-OH	3640-3670	[17]
Zr-O	470	[14]

The FTIR spectra show the absorption bands of silicate groups and aluminum ions, which characterize the aluminosilicate glass. The characteristic absorption band of Si-O-Si bonds is located at 467 and 473 cm<sup>-1</sup>[17]. The low absorption vibrations at 680 cm<sup>-1</sup>, and between 800 and 810 cm<sup>-1</sup> also indicate the presence of Si-O-Si bonds.

The glasses FTIR analysis shows the vibrations of amorphous Si-O bonds at 1070 cm<sup>-1</sup> [18]. These bands shift towards lower values, indicating the formation of Si-O-Me bonds (Me = Metal) in a crystallized structure. Me can be Mg or Al [19].

The characteristic bands of the annular structure of [SiO<sub>4</sub>] tetrahedra are observed at 750 cm<sup>-1</sup> and between 1000-1120 cm<sup>-1</sup>[20].

The contribution of the band centered at 444 cm<sup>-1</sup> indicates the presence of Na-O and K-O [21].

The vibration of Na and/or K cations appears at 467 cm<sup>-1</sup> [21].

The absorption bands at 470 cm<sup>-1</sup> correspond to Zr-OH vibrations [22]. A band between 443 and 460 cm<sup>-1</sup>, is attributed to the FeO<sub>4</sub> elongation vibration[23].

Thus, the band between 416 and 488cm<sup>-1</sup> corresponds to the vibration of ZrO<sub>6</sub> units [24].

The band at 750cm<sup>-1</sup> also confirms the presence of Si-O-Me bonds in the Si-Al-Me base glassy system (Me = Al or Mg) [25].

It is likely that the peak observed at 920 cm<sup>-1</sup> corresponds to the vibration of [AlO<sub>4</sub>] tetrahedral units.

The weak absorptions between 640 and 692 cm<sup>-1</sup> correspond to the elongation vibration of [AlO<sub>8</sub>] octahedra, and those at 839 cm<sup>-1</sup> to [AlO<sub>4</sub>] tetrahedra.

It is the same in the spectrum region of 1100-1200 cm<sup>-1</sup>, where the broadband observed may indicate [SiO<sub>4</sub>] tetrahedra.

The Al-OH elongation vibrations appear at 3640, 3660 and 3670 cm<sup>-1</sup>[26].

Both asymmetrical and symmetrical elongations of OH hydroxide group are always between 3700 and 3200 cm<sup>-1</sup>. The absorption bands around 3550, 3400 and 3250 cm<sup>-1</sup> represent the oxygen-hydrogen valence vibrations, of water molecule. The deformation frequencies of the later are between 1680 and 1622 cm<sup>-1</sup>.

The lower absorption bands of 1625 and 603 cm<sup>-1</sup> represent the Si-OH bond [26]. These latter groups represent the samples moisture.

We can conclude that the FTIR spectra are representative of the chemical composition of the studied glasses, and are similar to each other. They show that the glasses main functions do not depend on  $[Na_2O]/([Na_2O]+[Li_2O])$  ratio.

This proves that the microstructural changes due to the variations of  $[Na_2O]/([Na_2O]+[Li_2O])$  alkali molar ratio do not affect the presence of the functional groups of the glass chemical units.

### 3.3. Thermal characterization

The DTA analysis is performed by a Netzsch 409 PC, in the temperature interval of 20-1450 °C, for samples with  $[Na_2O]/([Na_2O]+[Li_2O])=0.057$  and 0.278 molar ratio. The glass transition (T<sub>g</sub>), crystallization (T<sub>c</sub>) and fusion (T<sub>f</sub>), temperatures are given in Table 3.

Table 3

Allotropic transformations of the glasses with  $[Na_2O]/([Na_2O]+[Li_2O])$  molar ratio=0.057 and 0.278.

$[Na_2O]/([Na_2O]+[Li_2O])$	T <sub>g</sub> (°C)	T <sub>c</sub> (°C)	T <sub>f</sub> (°C)
0.057	563.46	755.81	1280.06
0.278	666.42	779.13	1290.09

T<sub>g</sub> increases with  $[Na_2O]/([Na_2O]+[Li_2O])$  due to the formation of NBO oxygens in the glass network. It is strongly dependent on the nature of the cation network modifier. It is maximum when  $[Na_2O]/([Na_2O]+[Li_2O])$  molar ratio=0.278.

The presence of modifying cations into a silica glass has the effect of breaking Si-O-Si bonds and creating NBO oxygen, at the rate of one O per M<sup>+</sup> alkaline ion and two O per M<sup>2+</sup> alkaline

earth ions. Therefore, the modifying ions have the effect of depolymerizing the silicate network, and create discontinuities within it, by introducing ionic bonds ( $M + \dots NBO$  or  $M^{2+} \dots NBO$ ). As a consequence, the glassy network loses its rigidity. This reduces both the viscosity and melting temperature. As an example, the latter decreases from 1713 °C to about 800 °C for a glass of silica when 25% molar  $Na_2O$  is added [27].

This can explain the raise of  $T_g$ ,  $T_c$  and  $T_f$  with  $[Na_2O]/([Na_2O]+[Li_2O])$  molar ratio, in the present study.

In the present study,  $T_g$  values are higher than 450°C which is the radioactive waste package temperature. Thus, the studied glasses are suitable candidates for radioactive waste sequestration.

### 3.4. Mechanical characterization

#### Micro-hardness and Young's modulus measurements

The prepared glass samples are polished to mirror image and the micro-hardness was measured using micro-hardness indentations, with a force of 300 g for 10 s. The measurements were performed with a Zwick micro-durometer. Young's moduli are measured by RFDA (Resonant Frequency and Damping Analyzer) basic equipment, in bending mode, on rectangular bars. The results are given in Table 4.

Table 4

Glasses Vickers Hardness and Young's Modulus as a function of  $[Na_2O]/([Na_2O]+[Li_2O])$  molar ratio

$[Na_2O]/([Na_2O]+[Li_2O])$	Vickers Micro-hardness (HV)	Young's modulus (GPa)	
		E	$\Delta E$
0.057	741	1.62	0.13
0.121	749	2.23	0.12
0.194	661	2.36	0.11
0.278	569	2.06	0.17

Vickers micro-hardnesses vary between 569 and 749 HV. The estimated error on the values is about  $\pm 5$  HV. These results are in agreement with those of literature. N.P. Bansal and al. [28] reported non-linear values in the average of 431-508 HV for a silicate glass in the system  $Na_2O-Fe_2O_3-SiO_2$ . This behavior is due to  $[Na_2O]/([Na_2O]+[Li_2O])$  molar ratio variations, which are associated to the MAE effect.

The MAE affects Young's modulus values, which vary randomly between 1.62 and 2.36 GPa, with  $[Na_2O]/([Na_2O]+[Li_2O])$ . They increase with  $[Na_2O]/([Na_2O]+[Li_2O])$  up to the maximum value of 2.36 GPa, which correspond to  $[Na_2O]/([Na_2O]+[Li_2O])=0.194$ , where the equimolar condition is satisfied. Beyond this value, Young's modulus decreases.

The gap with the literature values are due to errors on RFDA measurements, attributed to both the samples small size and their surface roughness.

In general, the micro-hardness decreases with  $[Na_2O]/([Na_2O]+[Li_2O])$  molar ratio, when the Na content increases and Young's modulus increases as well. This can be due to a network expansion, provoked by the decrease of  $Li^+$  concentration in the glass. Such effect has been described by F.Pacaud and al.[29].

More than this, in Fe-rich silicate glasses, Na content has a low influence on the mechanical properties[30]. This emphasizes the idea that  $Li^+$  is responsible of the evolution of both the micro-hardness and Young's modulus.

J. Kjeldsen and al.[31] found Young's modulus between 6628 and 7444 HV for average Na/Li molar ratios of 0.05-1.0 %, for a  $SiO_2-Al_2O_3-MgO-CaO-Na_2O/K_2O$  glass. These high values show a good glass elasticity. Such a glass has a simple composition, compared to the presently studied glass. These authors noted a minimum of hardness for a maximum of plastic flow.

The nonlinear variations of both Microhardness and Young's modulus are due to the MAE effect.

### 3.5. Electrical characterization

The glasses resistivity for different  $[Na_2O]/([Na_2O]+[Li_2O])$  molar ratio are presented in Fig. 5.

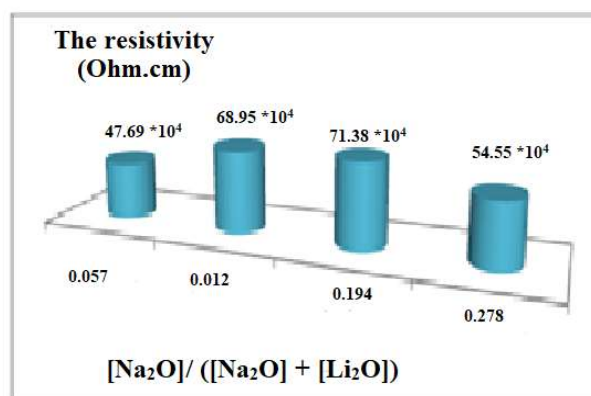


Fig. 5– The glass electrical resistivity as a function of  $[Na_2O]/([Na_2O]+[Li_2O])$  molar ratio.

The simultaneous presence of both Na and Li produces a maximum of resistivity when  $[Na_2O]/([Na_2O]+[Li_2O])=0.194$ . This corresponds to a minimum of electrical conductivity. The nonlinearity of the electrical resistivity is associated to the depolymerization of the glass network. In alkali aluminosilicates, this effect is less known.

The introduction of modifying cations into a silica glass has the effect of breaking Si-O-Si bonds and creating NBO oxygens. The

depolymerization, thus created, reduces the electrical conductivity of the vitreous network.

In addition, another parameter may explain this phenomenon, namely the ionic field form of alkaline element.

The polarizing effect of the cations depends on the field strength  $F = Z/a^2$  (where  $Z$  is the charge of the cation, and  $a$  the mean distance to oxygen atoms which is function of the cation coordination). This makes it possible to establish a classification of the different cations.

For example, the A.Dietzel criterion [32] indicates that the modifying ions are characterized by a weak strength field of less than 0.35 [33]. Because they have a low charge and both high ionic and coordination radii.

Other variants of field strength expression exist in the literature. For example, the cation-oxygen distance, equal to the sum of ionic radii of the cation and oxygen, can be replaced by the ionic radius  $r$  of the cation. This has a direct effect on the network's ability to conduct an electrical current.

In the present study, lithium, which has a higher average field strength compared to that of sodium, increases the conductivity MFS (mean field strength) of  $\text{Li} = 0.28 \text{ \AA}^{-2}$ , MFS of  $\text{Na} = 0.22 \text{ \AA}^{-2}$  [34]. Conversely, the electrical conductivity decreases when the  $\text{Li}^+$  content decreases.

The study of L. Pavic et al. [35] on aluminosilicate glasses electrical conductivity for  $[\text{Na}_2\text{O}]/([\text{Na}_2\text{O}]+[\text{K}_2\text{O}])$  and  $[\text{Na}_2\text{O}]/([\text{Na}_2\text{O}]+[\text{Li}_2\text{O}])$  molar ratios, reveals that the MAE effect is independent of Al content. Two main factors lead to this: the thermal ionic polarization and the electrode polarization [16].

#### 4. Conclusions

In this study, an aluminosilicate glass matrix is synthesized by a double melting at  $1450^\circ\text{C}$  by varying the amount of  $[\text{Na}_2\text{O}]/([\text{Na}_2\text{O}]+[\text{Li}_2\text{O}])$  molar ratio from 0.057 to 0.278. The Archimedes density and molar volume vary nonlinearly with  $[\text{Na}_2\text{O}]/([\text{Na}_2\text{O}]+[\text{Li}_2\text{O}])$  molar ratio, which show a MAE effect in the studied glass system. XRD analysis indicates the glasses amorphous nature, confirmed by SEM observations. The FTIR analysis reveals the main glass bounds.

DTA analysis gave  $T_g$  values higher than the radioactive waste package temperature during the earlier stages of storage, making the present glass a suitable candidate for radioactive waste confinement.

As for density, the microhardness and Young's modulus vary nonlinearly with  $[\text{Na}_2\text{O}]/([\text{Na}_2\text{O}]+[\text{Li}_2\text{O}])$  molar ratio. This behavior is associated to the network depolymerization (change in NOB concentrations), caused by the MAE. The mixture of Na and Li in the glass produces a maximum of resistivity when molar ratio

$[\text{Na}_2\text{O}]/([\text{Na}_2\text{O}]+[\text{Li}_2\text{O}])=0.194$ , which corresponds to a minimum of electrical conductivity.

#### REFERENCES

1. M.I. Ojovan, W.E. Lee, Glassy wasteforms for nuclear waste immobilization. Metallurgical and Materials Transactions A, 2011, **42**(4), 837.
2. M. I. Ojovan, W.E. Lee, An Introduction to Nuclear Waste Immobilisation, 1<sup>st</sup> Edition Elsevier Science Publishers B.V, Amsterdam, 2005, 315.
3. D. Holland, A. Mekki, I. A. Gee, C. F. McConville, J. A. Johnson, C. E. Johnson, P. Appleyard, and M. Thomas, The structure of sodium iron silicate glass—a multi-technique approach, Journal of non-crystalline solids, 1999, **253**(1), 192.
4. L. Chomat, Compréhension de l'altération à long terme des colis de verre R7T7: étude du couplage chimie transport dans un milieu fissuré, Thesis, Paris VI Pierre and Marie Curie University, Paris, 2008.
5. D.E. Day, Mixed alkali glasses—their properties and uses. Journal of Non-Crystalline Solids, 1976, **21**(3), 343.
6. M.D. Ingram, Ionic conductivity in glass. Physics and Chemistry of glasses, 1987, **28**(6), 215.
7. M.D. Ingram, B. Roling, The concept of matrix-mediated coupling: a new interpretation of mixed-cation effects in glass. Journal of Physics: Condensed Matter, 2003, **15**(16), 1595.
8. N. Ollier, B. Boizot, B. Reynard, D. Ghaleb, and G. Petite,  $\beta$  irradiation in borosilicate glasses: the role of the mixed alkali effect. Nuclear Instruments and Methods in Physics Research Section B: Beam Interactions with Materials and Atoms, 2004, **218**, 176.
9. A. Edukondalu, B. Kavitha, A. Hameed, and K.S. Kumar, Physical and optical studies on  $\text{Li}_2\text{O}-\text{Na}_2\text{O}-\text{WO}_3-\text{B}_2\text{O}_3$  glasses. In IOP Conference Series: Materials Science and Engineering 2015, **73**(1), 012127.
10. G. Padmaja, P. Kistaiah, Infrared and Raman spectroscopic studies on alkali borate glasses: evidence of mixed alkali effect. The Journal of Physical Chemistry A, 2009, **113**(11), 2397.
11. R. Laopaiboon, C. Bootjomchai, Radiation effects on structural properties of glass by using ultrasonic techniques and FTIR spectroscopy: a comparison between local sand and  $\text{SiO}_2$ . Annals of Nuclear Energy, 2014, **68**, 220.
12. R.L. Myuller, Electrical conductivity of solid Ionic –Atomic Valent Substances. X Electrical conductivity of Glasses Containing two kinds of Alkali Ions, Soviet physics. Technical physics, 1959, **4** (11), 1219.
13. J.F. Emerson, P.E. Stallworth, P.J. Bray, - High field  $^{29}\text{Si}$  NMR studies of alkali silicate glasses, Journal of Non-Crystalline Solids, 1989, **113**(2–3), 253.
14. T. Yano, S. Shibata, T. Maehara, Structural Equilibria in Silicate Glass Melts Investigated by Raman Spectroscopy, Journal of the American Ceramic Society, 2006, **89**(1), 89.
15. I. Yasui, H. Hasegawa, M. Imoaka, X-ray diffraction study of the structure of silicate glasses. Pt. 1: alkali metasilicate glasses, Physics and Chemistry of Glasses, 1983, **24**, 65.
16. H. Scholze, Le verre. Nature, structure et propriétés 2<sup>nd</sup> Ed, éditée by The Glass Institute, Paris, 1980.
17. B.J. Saikia, G. Parthasarathy, Fourier transform infrared spectroscopic characterization of kaolinite from Assam and Meghalaya, Northeastern India. Journal of Modern Physics, 2010, **1**(4), 206.
18. N. Nagai, H. Hashimoto, FT-IR-ATR study of depth profile of  $\text{SiO}_2$  ultra-thin films. Applied surface science, 2001, **172**(3), 307.
19. R. Kaur, S. Singh, O.P. Pandey, FTIR structural investigation of gamma irradiated  $\text{BaO}-\text{Na}_2\text{O}-\text{B}_2\text{O}_3-\text{SiO}_2$  glasses, Physica B: Condensed Matter, 2012, **407**(24), 4765.
20. S. Atalay, H.I. Adiguzel, F. Atalay, Infrared absorption study of  $\text{Fe}_2\text{O}_3-\text{CaO}-\text{SiO}_2$  glass ceramics, Materials Science and Engineering: A, 2001, **304**, 796.
21. A. Edukondalu, C. Srinivasu, S. Rahman, K. S. kumar, Infrared and Raman Spectroscopic Studies on mixed alkali tungsten based glasses, International Journal of Scientific and Engineering Research, 2014, **5**(3), 258.

22. I.H. Joe, A.K.Vasudevan, G. Aruldas, A.D. Damodaran, K.G.K Warriar, FTIR as a Tool to Study High-Temperature Phase Formation in Sol–Gel Aluminium Titanate, Journal of Solid State Chemistry, 1997, **131**(1),181.
23. D.A Magdas, O. Cozar, V. Chis, I. Ardelean, N. Vedeanu, The structural dual role of Fe<sub>2</sub>O<sub>3</sub> in some lead-phosphate glasses, Vibrational Spectroscopy, 2008, **48**(2),251.
24. P. Pascuta, G. Borodi, N. Jumate, I. Vida-Simiti, D. Viorel, E. Culea, The structural role of manganese ions in some zinc phosphate glasses and glass ceramics, Journal of Alloys and Compounds, 2010, **504**(2),479.
25. M. Sales, J. Alarson, Crystallization of sol-gel derived glass ceramic powders in the CaO-MgO-Al<sub>2</sub>O<sub>3</sub> - SiO<sub>2</sub> system. Part II: Cordierite, Journal of Materials Science, 1995, **30**(9),2341.
26. R. Palanivel, G. Velraj : FTIR and FT-Raman spectroscopic studies of fired clay artifacts recently excavated in Tamilnadu, India, 2007, **45**, 501.
27. J.F. Emerson, P.E. Stallworth, P.J. Bray, - High field 29Si NMR studies of alkali silicate glasses , Journal of Non-Crystalline Solids, 1989, **113**(2–3),253.
28. N.P. Bansal, R.H. Doremus, Handbook of Glass Properties, United Kingdom, Edited by Academic Press INC, Orlando, USA, 1986).
29. F.Pacaud, C. Fillet, G. Baudin, H. Bastien-Thiry, in Proceedings of the 2<sup>nd</sup> International Seminar on radioactive Waste Products. (Julich Germany, May 1990), p. 577.
30. D.J.M. Burkhard, Iron-bearing silicate glasses at ambient conditions, Journal Non Crystalline Solids, 2000, **275**,175.
31. J. Kjeldsen, M.M. Smedskjaer, J.C. Mauro, Y. Yue, On the origin of the mixed alkali effect on indentation in silicate glasses. Journal of Non-Crystalline Solids, 2014, **406**, 22.
32. A. Dietzel, Die Kationenfeldstärken und ihre Beziehungen zu Entglasungsvorgängen, zur Verbindungsbildung und zu den Schmelzpunkten von Silicaten, Berichte der Bunsengesellschaft für physikalische Chemie, 1942, **48**(1), 9.
33. J. Barton, C. Guillemet, Le verre. Science et Technologie, edited by EDP Sciences, Les Ulis, 2005) p.442.
34. G.E. Brown Jr., F. Farges, Calas G., in: J. F. Stebbins, P.F. McMillan, D. B. Dingwell, (edited by Structure, Dynamics and Properties of Silicate Melts, Reviews in Mineralogy, (32), (The Mineralogical Society of America, Washington DC, 1995), p. 615.
35. L. Pavic, A. Moguš-Milankovic, P. Raghava Rao, A. Šantic, V. Ravi Kumar, N. Veeraiah, Effect of alkali-earth modifier ion on electrical, dielectric and spectroscopic properties of Fe<sub>2</sub>O<sub>3</sub> doped Na<sub>2</sub>SO<sub>4</sub>—MO—P<sub>2</sub>O<sub>5</sub> glass system. Journal of Alloys and Compounds, 2014, **604**, p.352.

\*\*\*\*\*

## MANIFESTĂRI ȘTIINȚIFICE / SCIENTIFIC EVENTS



**China Glass**  
**22-25 May 2019**  
**China International Exhibition Center,**  
**Beijing China**

**"International exhibition for glass processing technology"**

The China Glass is a dedicated trade show that offers industry professionals with matchless opportunities and insights into China vibrant glass industry. It brings together exhibitors from around the world and provides them with the opportunity to display the latest in glass products, services, solutions and technologies and provides an analysis of existing and future trends relating to the glass industry.

**Contact:** [ceramsoc@chinaglass-exp.com](mailto:ceramsoc@chinaglass-exp.com)

\*\*\*\*\*